MAXIMUM-LIFT AND STALLING CHARACTERISTICS OF WINGS

By James C. Sivells

Langley Aeronautical Laboratory

The maximum-lift and stalling characteristics of wings constitute a subject that is common to all types of airplanes, small or large, low speed or high speed. The problems associated with each type may, however, be widely different. The old biplanes and early monoplanes had stalling characteristics which were usually fairly good. The wing loadings were low so that the landing speeds were relatively low. The relatively thick, rectangular wings tended to stall near the center and gave the pilots adequate stall warning. As the airplane designs became more efficient, the structural designers demanded that the wings be tapered to decrease the stresses at the wing roots. Tapering the wings, however, tended to move outboard the spanwise position of the incipient stall, so that a compromise has to be made between the structural and aerodynamic desiderations. Recently the use of thinner and smoother wing sections, higher wing loadings, and unconventional plan forms has resulted in further compromises, both structural and aerodynamic, since the factors which are necessary for high-speed performance are usually not conducive to low-speed performance. All present-day airplanes represent the results of such compromises which have been made in their designs.

Since it is desirable to be able to predict the maximum-lift and stalling characteristics of an airplane at a very early stage in its design, a large amount of research has been done with this end in mind. This research has been undertaken along three lines - theoretical work, wind-tunnel experiments, and flight tests - which must be closely correlated to provide the maximum amount of useful information. The theoretical work can indicate trends due to variations in the wing geometry but cannot adequately include the interference effects of the fuselage or nacelles. The wind-tunnel experiments can determine the maximum lift values for a smooth model or one with standard leading-edge roughness but oftentimes at values of Reynolds number or Mach number different than those at which the airplane will fly. Moreover, the stalling characteristics determined in most wind tunnels are obtained for models which are restrained at a given attitude so that the motions of a stalled airplane cannot be simulated. The final analysis of the maximum-lift and stalling characteristics of an airplane comes in the flight tests where all the factors which influence the characteristics are integrated. At this stage of the design, however, it may be too late or very expensive to make alterations necessary to improve the characteristics. In spite of all the research which has been done along these lines, much more remains to be done before accurate predictions can be made of the characteristics of every type of airplane.

One of the major factors which influence the maximum-lift and stalling characteristics of a wing is its airfoil section. Comparisons

of various airfoil sections can best be made from the results of two-dimensional wind-tunnel tests. The NACA 6-series airfoil sections have been described in the paper by von Doenhoff and Loftin. In figure 1, the values of the maximum lift coefficient of the NACA 64-series sections are shown for a Reynolds number of 6×10^6. (See reference 1.) In order to provide an indication of the maximum-lift capabilities of an airfoil with various types of high-lift flaps, nearly all sections are tested with and without 20-percent-chord split flaps deflected 60°. Varying the airfoil thickness ratio has approximately the same effect on the maximum lift of the NACA 6-series airfoils as it does on the older 4- and 5-digit airfoil sections. (See reference 2.) Without flaps, the highest values are for thickness ratios of about 12 to 15 percent. With flaps, the highest values are for thickness ratios of about 18 to 21 percent. The airfoil thickness also has an appreciable effect on the sharpness of the lift-curve peak (reference 3) which, in turn, may influence the stalling characteristics of a wing. The very thin sections, up to about 6 percent thick, have flat-top lift curves, characteristic of flat plates. The sections from about 9 to 12 percent thick have relatively sharp-peak lift curves characterized by abrupt separation of the flow from the entire upper surface initiated by laminar separation near the leading edge. The actual flow mechanism is quite complex but is described more fully in reference 3. The thicker sections have more rounded lift-curve peaks characterized by separation of the turbulent boundary layer starting at the trailing edge. Not only the thickness but also the airfoil contour, particularly the forward part, has an effect on the section stalling characteristics so that different families of airfoils do not necessarily exhibit the same characteristics. For example, for equal thicknesses, the NACA 6-series sections do not have as sharp lift-curve peaks as the NACA 230-series sections.

The addition of camber of the uniform-load type generally increases the values of maximum lift coefficient as shown in figure 1 for values of design lift coefficient c_{l_i} of 0.2 and 0.4. Still greater amounts of camber do not further increase the maximum lift coefficient. These curves are typical of all the NACA 6-series sections. The values for NACA 63-series sections are generally a little higher than those shown while those for the NACA 65- and 66-series are a little lower. The effects of Reynolds number on the values of maximum lift coefficient are about the same as for the older types of airfoils. These data were all obtained with the airfoils in a smooth condition. With so-called standard leading-edge roughness applied to the forward 8 percent of the airfoil surface, the effects of thickness and Reynolds number are materially reduced. For example, at the Reynolds number of 6×10^6, the values of maximum lift coefficient for the 6-percent-thick sections are little affected by roughness, for the 12-percent-thick sections losses of 0.3 to 0.5 are caused by roughness, and for the thicker sections the losses due to roughness are of the order of 0.2 to 0.3. These losses in $c_{l_{max}}$ are accompanied by a rounding-off of the lift-curve peaks.

The thicker sections with split flaps give fairly high values of maximum lift coefficient, of the order of 2.8. For high-speed performance, however, much thinner sections must be used, usually less than 12 percent thick. It then becomes imperative to use some more powerful type of high-lift device in order to obtain high values of maximum lift coefficient. In figure 2 are shown typical values which can be obtained for various types and combinations of high-lift devices. The difference between the two sections shown is mainly that of camber. The double slotted flap is one of the most powerful types of trailing-edge flap and on the NACA 64_1A212 section produces a value of $c_{l_{max}}$ of about 2.85 for a Reynolds number of 6×10^6 as compared with a value of 2.41 obtained with a split flap. (See references 4 and 5.) The addition of a leading-edge slat increases the value of $c_{l_{max}}$ to about 3.38. A still further increase can be obtained by removing part of the boundary layer by suction through one or more slots. For a single slot located at 40 percent of the chord and a flow coefficient of 0.025, a maximum lift coefficient of 3.72 has been obtained in conjunction with a double slotted flap and a leading-edge slat.

Another type of leading-edge device is the extensible leading-edge flap. (See reference 6.) Two types of flap are shown with the NACA 64_1-012 section; one is intended to be hinged at the lower surface near the nose of the airfoil and the other is intended to be retracted into the upper surface. The lower-surface flap is probably simpler from a construction standpoint but produces a discontinuity at the nose and is, therefore, not as effective as the upper-surface flap. Used in conjunction with a split flap, however, the lower-surface leading-edge flap produces a fairly high value of $c_{l_{max}}$ One advantage of the leading-edge flap as a high-lift device is that it produces approximately the same values of $c_{l_{max}}$ on still thinner airfoil sections (reference 7) even though the values obtained for the plain airfoil decrease rapidly with decreasing thickness.

Although the two-dimensional data give a fairly good indication of the relative merits of various airfoil sections, the other factors which influence the maximum-lift and stalling characteristics of wings must be investigated in three-dimensional flow on wings of finite span. Complete wings may be divided into two catagories: those having little or no sweep and those which are sweptback or sweptforward enough that the sweep has an influence on the wing characteristics. Since much more is known about the characteristics of unswept wings, these are discussed first.

Except for wings of very low aspect ratio, the various sections of an unswept wing behave very much as they do in two-dimensional flow but at an effective angle of attack as predicted by lifting-line theory. Even the nonlinearity of the section lift curves in the vicinity of

maximum lift can be taken into account by a method developed for calculating the wing characteristics using actual two-dimensional data. (See reference 8.) Figure 3 shows the results of such calculations for one of a series of wings. (See references 9 to 11.) The calculated curve is here superimposed on the points obtained experimentally. This particular wing has the fairly high aspect ratio of 10 and a taper ratio of 0.4. The sections varied in thickness from 20 percent at the root to 12 percent at the tip and account was taken of the variation in Reynolds number from root to tip due to the taper. The agreement between the calculated and experimental results was very good for this wing and at least reasonably good for all the wings of the series investigated. In all cases the agreement was better than if no account were taken of the nonlinearity of the section lift curves.

In addition to the value of the maximum lift coefficient, the stalling characteristics of a wing can be predicted by this method as shown in figure 4. This is for the same wing as the previous figure. The upper, or dotted, curve shows the spanwise variation of the maximum lift coefficient for the various sections as determined from two-dimensional tests. The variations of thickness and Reynolds number along the span are taken into account. The lower, or solid, curve is the spanwise variation of the local section lift coefficient at the maximum value of wing lift coefficient as calculated by the method mentioned. Where the curves are tangent, the sections have reached their maximum values of lift coefficient and the stall has begun. The divergence between the curves is an indication of the progression of the stall. In this particular case, the difference between the curves at the root is probably insufficient to prevent separation, so that the wing would be predicted to be stalled over about 90 percent of the semispan. From wind-tunnel tests with tufts attached to the wing, the area indicated was stalled at maximum lift. The agreement between the wind-tunnel tests and the predicted stall is reasonable. Whether this wing would have satisfactory stalling characteristics in flight cannot be predicted from these data inasmuch as the motions of the stalled airplane are not known. It can be conjectured that some loss in aileron effectiveness would be experienced near maximum lift but, because of the thick root sections which experience separated flow at values of lift coefficient somewhat below the maximum, the pilot may have warning of the incipient stall in the nature of tail buffeting.

Although the maximum-lift and stalling characteristics of unswept wings are believed to be predicted better by the method using nonlinear section lift data than by older methods in which the section lift curves are assumed to be linear, much useful information has been obtained by the latter methods as to the effects of various geometric parameters. One such theoretical investigation (references 12 and 13) provides the information shown in figure 5. It has been generally accepted that a rectangular wing (taper ratio of 1) will possess good stalling characteristics inasmuch as the stall tends to start at the root and progress slowly outboard as indicated by the lower left-hand curves. There may be certain combinations of variables, however, for which such a

generalization is not true. Furthermore, too early a root stall may seriously reduce the maximum lift or cause too much tail buffeting. It may, therefore, be desirable from an aerodynamic as well as a structural standpoint to taper the wing. A taper ratio of 1/2, which many designers consider to be moderate, moves the incipient-stall position dangerously far outboard for a wing with this particular combination of airfoil sections. If other design criterions allow the root thickness to be increased to 21 percent, the stall can again be moved inboard because the thicker sections have lower values of $c_{l_{max}}$. It is thus readily seen that it is extremely important to consider not only the taper ratio but also the airfoil section and other variables in the design of a wing with good stalling characteristics. The lower right-hand curves show that more taper again shifts the stall outboard even though the root section is quite thick.

A few general remarks should be made at this time. The use of nonlinear section lift data has oftentimes indicated that the stall would be more severe than that indicated by the use of linear data. These four examples shown are for an aspect ratio of 6, constant camber from root to tip, and no washout. The effect of increasing aspect ratio is to level off the local-lift-coefficient distributions thereby making the stalling characteristics better or worse depending upon the shape of the maximum-section-lift-coefficient distribution. An increase in camber from root to tip will usually improve the stalling characteristics if the maximum section lift coefficients are increased near the tip. Washout will also improve the stalling characteristics by increasing the local lift coefficients near the root and decreasing them near the tip. The use of either camber increase or washout may be limited, however, by the high-speed requirements for the airplane. The high-speed requirements may also dictate the shape and thickness of the airfoil section which may greatly influence the stalling characteristics in a manner not shown in the above type of analysis or even in wind-tunnel tests. The use of an airfoil section with a sharp-peak lift curve may result in a rapid roll-off or pitching motion when the airplane stalls in flight. Another factor which may affect the stalling characteristics of an airplane is the slipstream from a tractor propeller. (See reference 14.) The increased velocity in the slipstream increases the local Reynolds number of the wing sections behind the propeller. The downwash behind an inclined propeller tends to reduce the effective angle of attack of the wing sections. Both of these effects tend to delay stalling in the affected regions and may allow the outboard sections of the wing to stall first. Another effect is that of slipstream rotation which causes the sections behind the upgoing propeller blades to stall before the sections behind the downgoing propeller blades.

Where the high-speed requirements influence the design so that a poor-stalling wing results, the designer may resort to the use of stall control devices such as the sharp leading edge and leading-edge slat.

Figure 6 shows the use of a sharp leading edge on a wing with a taper ratio of 1/3. (See reference 15.) The outboard stall of the plain wing is corrected by decreasing the maximum section lift coefficients near the root; the stall is thereby caused to move inboard. The use of this type of stall control device results in a lower maximum lift coefficient of the wing and would probably not be used except where absolutely necessary. Figure 7 shows the use of a leading-edge slat over the outboard part of the wing. (See reference 12.) In this case the tip stall is prevented by increasing the maximum-lift capabilities of the outboard sections and a higher wing lift is obtained. Although this analysis indicates that the stall would be localized near the inboard end of the flap, it is extremely difficult to predict the flight characteristics.

Associated with the maximum-lift and stalling characteristics of airplanes is the sinking speed in the landing approach. This may be a deciding factor as to what type of high-lift device to use. Figure 8 shows the lift-drag polars of a wing-fuselage combination with three types of 60-percent-span flaps. (See reference 16.) To place the flaps on a more comparable basis, a tail length was assumed and the negative lift on the tail, necessary to trim out the pitching moment due to the flaps, was added to the wing lift to give a value of trimmed lift coefficient. Superimposed on these polars is a grid of lines of constant sinking speed V_v and constant gliding speed calculated for a wing loading of 60 pounds per square foot. Although neither the drag of nacelles, landing gear, tail, and protuberances nor the effects of power is included, a comparison of the various types of flap can be made. The lowest sinking speed for any of the flapped-wing configurations would be obtained with the single slotted flaps but the lowest gliding speed would be obtained with the double slotted flaps. These data are for a 10-percent-thick wing with an aspect ratio of 9. For this particular wing, the flaps had practically no effect on the stalling characteristics.

In the estimation of full-scale flight values of maximum lift coefficient from wind-tunnel data, due account must be taken of the difference in Mach number as well as the difference in Reynolds number between the flight and wind-tunnel conditions. Although the effects of compressibility are usually associated with relatively high subsonic Mach numbers, such effects are also important at Mach numbers as low as 0.2 in studies of maximum lift. Some of the interrelated effects of Mach number and Reynolds number are shown in figure 9. (See reference 17.) These data were obtained by testing the same wing at atmospheric pressure and at a pressure of about $2\frac{1}{4}$ atmospheres. At each pressure, tests were made over the range of Mach number. The same data are plotted as a function of both Reynolds number and Mach number. The peak values of maximum lift coefficient in each case were obtained when the critical pressure coefficient, corresponding to a local Mach number of 1, was reached. At speeds lower than this critical speed, the Reynolds number had more effect; $c_{l_{max}}$ increased with increasing Reynolds number. At speeds higher than

the critical speed, Mach number had more effect; $c_{l_{max}}$ decreased with increasing Mach number. At the higher Reynolds number, the pressure coefficients were more negative and the critical pressure coefficient was reached at a lower free-stream Mach number. The pressure coefficients were still more negative with the flaps deflected and the critical pressure coefficient was reached at still lower free-stream Mach numbers. Although these data pertain to one particular wing, they do show the importance of considering both the Reynolds number and the Mach number when estimations are made of the maximum lift coefficient of a wing.

Up to this point, only unswept wings have been considered. Although many of the factors which influence the maximum-lift and stalling characteristics of unswept wings also affect the characteristics of swept wings, such effects are often masked by the effect of sweep. The characteristics of swept wings are not as amenable to calculation as those of unswept wings. Some qualitative effects of sweep, however, may be discussed. As shown in the previous paper by Toll and Diederich from calculations by lifting-surface theory, sweepback tends to load up the outboard sections of a wing while sweepforward tends to load up the inboard sections. In addition to these effects on the span loading, the spanwise component of the air flow tends to sweep the boundary layer outboard on sweptback wings and inboard on sweptforward wings. The thickened boundary layer which results is more susceptible to separation than the thinner boundary layer on an unswept wing. The effects are additive, causing severe tip stall on sweptback wings and severe root stall on sweptforward wings as shown in figure 10. (See reference 18.) For these tests the same semispan wing was rotated to give the various angles of sweep, and different tip and root sections were added for each angle. The aspect ratio was thus decreased as the sweep was increased. In addition to the loss in lateral control at the stall of the sweptback wings, sweep, either forward or backward, may cause longitudinal instability at the stall for some aspect ratios. This is discussed more fully in another paper but is mentioned here because subsequent values of maximum lift shown may not be usable because of longitudinal instability.

The effect of sweepback on maximum lift coefficient is shown in figure 11. (See reference 19.) These results were obtained in a turbulent wind tunnel and the values of Reynolds number are the so-called "effective" values obtained by multiplying the test values by a factor which is a function of the amount of turbulence in the air stream. The validity of the use of this concept of effective Reynolds number has not been established for swept wings. The important point shown by these curves is that Reynolds number must be taken into account when discussing the effect of sweep on the maximum lift coefficient of a wing and low-scale wind-tunnel results may not apply to full-scale airplanes.

Sweep also has a pronounced effect upon the increment in lift coefficient due to flap deflection as shown in figure 12. (See reference 20.) These are low-scale results obtained at a Reynolds number

of 1×10^6 to 2×10^6. All the wings tested had the same chord normal to the leading edge, were untapered, and had the same span. The aspect ratio decreased, therefore, with increasing sweepback. The increment in lift coefficient is due to the deflection of 50-percent-span, 20-percent-chord, split flaps deflected 60°. At low angles of attack, the increment in lift coefficient varies approximately as the empirical cosine-squared curve multiplied by the factor η to take into account the difference in aspect ratio. The increment in maximum lift coefficient is somewhat lower, falling to zero for 60° sweepback.

As mentioned previously, the tip stall of a sweptback wing causes a loss in lateral control and may cause longitudinal instability. It is oftentimes possible, however, to eliminate this tip stall by some stall control device. Figure 13 shows the results of using partial-span, properly located, leading-edge slats on a highly tapered, moderately sweptback wing. (See reference 14.) In this case, not only was the tip stall eliminated, but the maximum lift coefficient was increased by the addition of the slats. It should be re-emphasized that the slats must be properly located both as to span and position to improve the stalling characteristics of such a wing because improperly located slats on this same model did not give any improvement.

In conclusion, the present status and future needs of research on maximum-lift and stalling characteristics can be summarized. Theoretical methods of analysis for unswept wings have been developed for predicting the effects of variations in wing geometry. Similar methods are needed which can include the effects of sweep and low aspect ratio. Wind-tunnel experiments have been useful for determining some of the effects of sweep and of various airplane components. Further wind-tunnel investigations are desirable in which the models are allowed some degree of freedom, such as rolling, so that flight conditions can be partly simulated. Further flight tests are desirable for investigating the effects of variables which cannot be taken into account at present either by theory or in the wind tunnels and for defining more nearly exactly what are satisfactory stalling characteristics. Finally, close correlation must be maintained between the theoretical analyses, wind-tunnel experiments, and flight tests so that the information from each field of research can be applied to the others.

REFERENCES

1. Cahill, Jones F.: Summary of Section Data on Trailing-Edge High-Lift Devices. NACA RM No. L8D09, 1948.

2. Abbott, Ira H., Von Doenhoff, Albert E., and Stivers, Louis S., Jr.: Summary of Airfoil Data. NACA Rep. No. 824, 1945.

3. Jacobs, Eastman N., and Sherman, Albert: Airfoil Section Characteristics as Affected by Variations of the Reynolds Number. NACA Rep. No. 586, 1937.

4. Quinn, John H., Jr.: Tests of the NACA 64_1A212 Airfoil Section with a Slat, a Double Slotted Flap, and Boundary-Layer Control by Suction. NACA TN No. 1293, 1947.

5. Loftin, Laurence K., Jr.: Theoretical and Experimental Data for a Number of NACA 6A-Series Airfoil Sections. NACA TN No. 1368, 1947.

6. Fullmer, Felicien F., Jr.: Two-Dimensional Wind-Tunnel Investigation of the NACA 64_1-012 Airfoil Equipped with Two Types of Leading-Edge Flap. NACA TN No. 1277, 1947.

7. Fullmer, Felicien F., Jr.: Two-Dimensional Wind-Tunnel Investigation of an NACA 64-009 Airfoil Equipped with Two Types of Leading-Edge Flap. NACA TN No. 1624, 1948.

8. Sivells, James C., and Neely, Robert H.: Method for Calculating Wing Characteristics by Lifting-Line Theory Using Nonlinear Section Lift Data. NACA TN No. 1269, 1947.

9. Bollech, Thomas V.: Experimental and Calculated Characteristics of Several High-Aspect-Ratio Tapered Wings Incorporating NACA 44-Series, 230-Series, and Low-Drag 64-Series Sections. NACA TN No. 1677, 1948.

10. Sivells, James C.: Experimental and Calculated Characteristics of Three Wings of NACA 64-210 and 65-210 Airfoil Sections with and without 2° Washout. NACA TN No. 1422, 1947.

11. Neely, Robert H., Bollech, Thomas V., Westrick, Gertrude C., and Graham, Robert R.: Experimental and Calculated Characteristics of Several NACA 44-Series Wings with Aspect Ratios of 8, 10, and 12 and Taper Ratios of 2.5 and 3.5. NACA TN No. 1270, 1947.

12. Soulé, H. A., and Anderson, R. F.: Design Charts Relating to the Stalling of Tapered Wings. NACA Rep. No. 703, 1940.

13. Harmon, Sidney M.: Additional Design Charts Relating to the Stalling of Tapered Wings. NACA ARR, Jan. 1943.

14. Sweberg, Harold H., and Dingeldein, Richard C.: Summary of Measurements in Langley Full-Scale Tunnel of Maximum Lift Coefficients and Stalling Characteristics of Airplanes. NACA Rep. No. 829, 1945.

15. Anderson, Raymond F.: A Comparison of Several Tapered Wings Designed to Avoid Tip Stalling. NACA TN No. 713, 1939.

16. Sivells, James C., and Spooner, Stanley H.: Investigation in the Langley 19-Foot Pressure Tunnel of Two Wings of NACA 65-210 and 64-210 Airfoil Sections with Various Type Flaps. NACA TN No. 1579, 1948.

17. Furlong, G. Chester, and Fitzpatrick, James E.: Effects of Mach Number and Reynolds Number on the Maximum Lift Coefficient of a Wing of NACA 230-Series Airfoil Sections. NACA TN No. 1299, 1947.

18. Hieser, Gerald: Tuft Studies of the Flow over a Wing at Four Angles of Sweep. NACA RM No. L7C05a, 1947.

19. Anderson, Raymond F.: Determination of the Characteristics of Tapered Wings. NACA Rep. No. 572, 1936.

20. Letko, William, and Goodman, Alex: Preliminary Wind-Tunnel Investigation at Low Speed of Stability and Control Characteristics of Swept-Back Wings. NACA TN No. 1046, 1946.

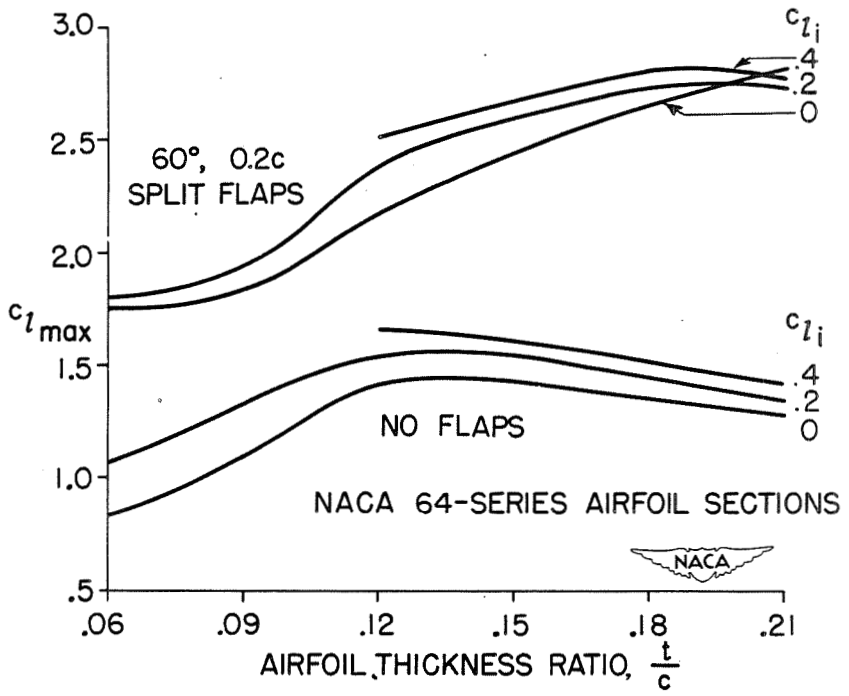

Figure 1.- Maximum-lift characteristics of NACA 64-series airfoil sections at a Reynolds number of 6×10^6.

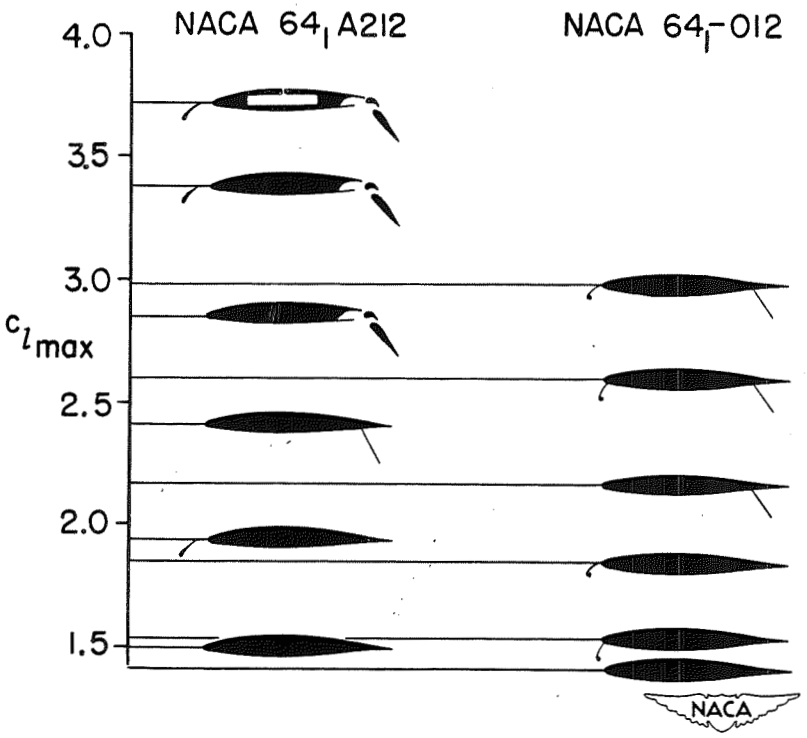

Figure 2.- Maximum lift coefficients of NACA 64_1A212 and 64_1-012 airfoil sections with various high-lift devices. Reynolds number, 6×10^6.

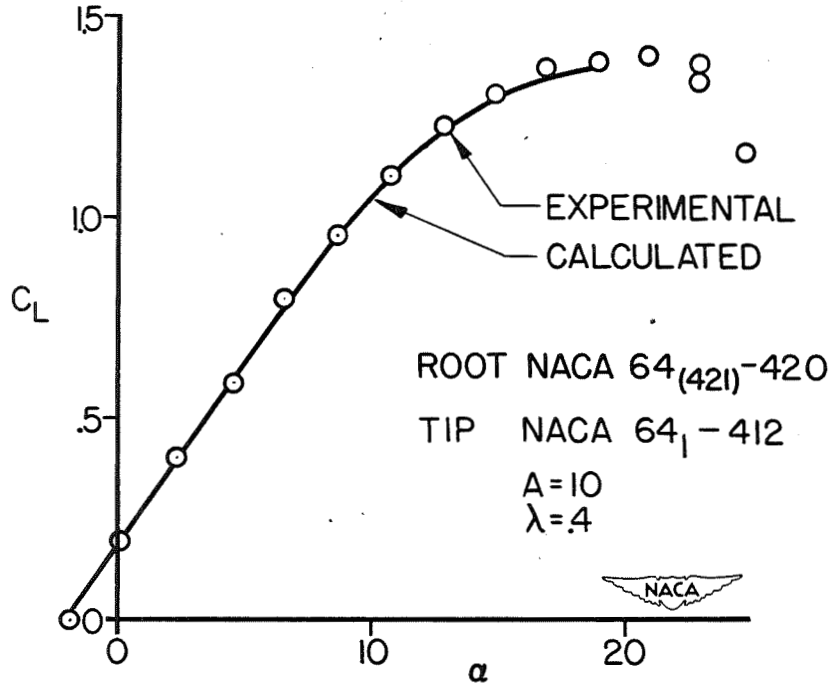

Figure 3.- Experimental and calculated maximum-lift characteristics of a wing with NACA 64-series sections.

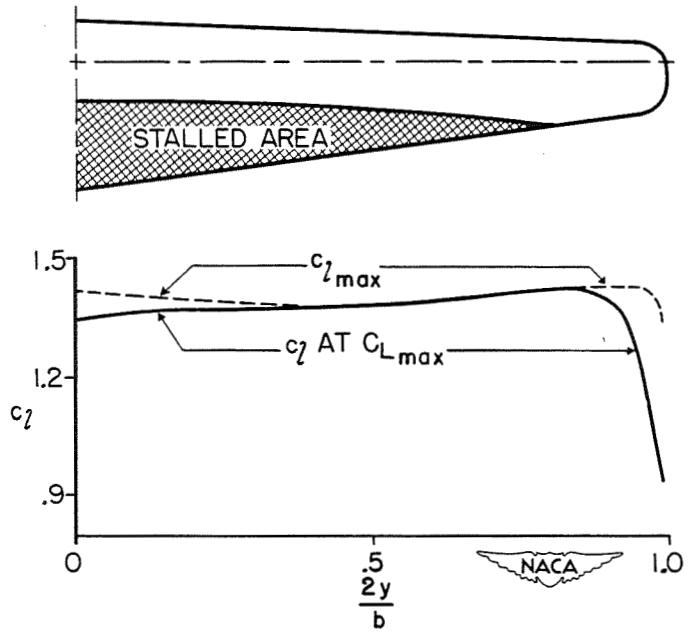

Figure 4.- Experimental and calculated stalling characteristics of a wing with NACA 64-series sections.

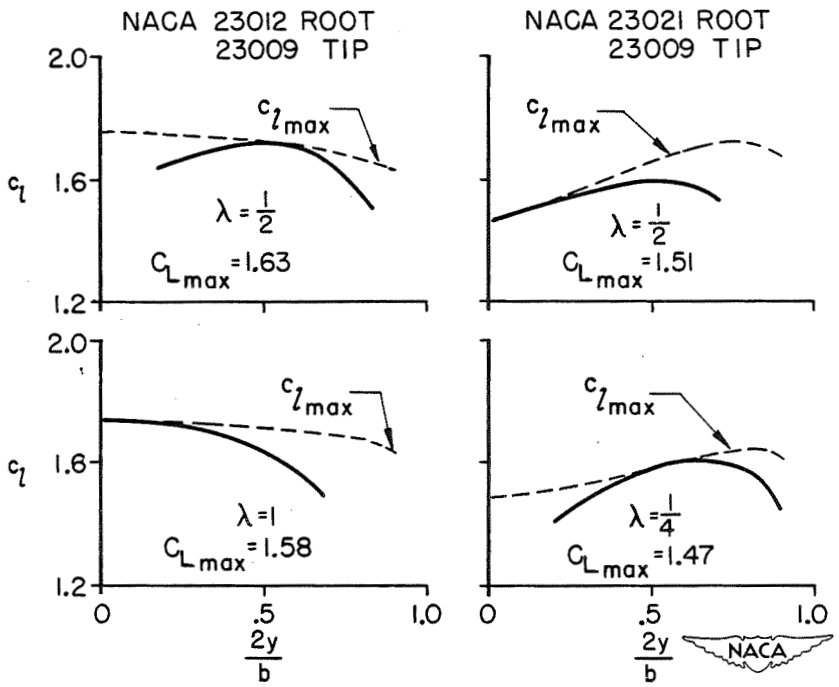

Figure 5.- Spanwise lift-coefficient distributions at maximum lift for four wings with NACA 230-series sections. Aspect ratio, 6; Reynolds number, 8×10^6.

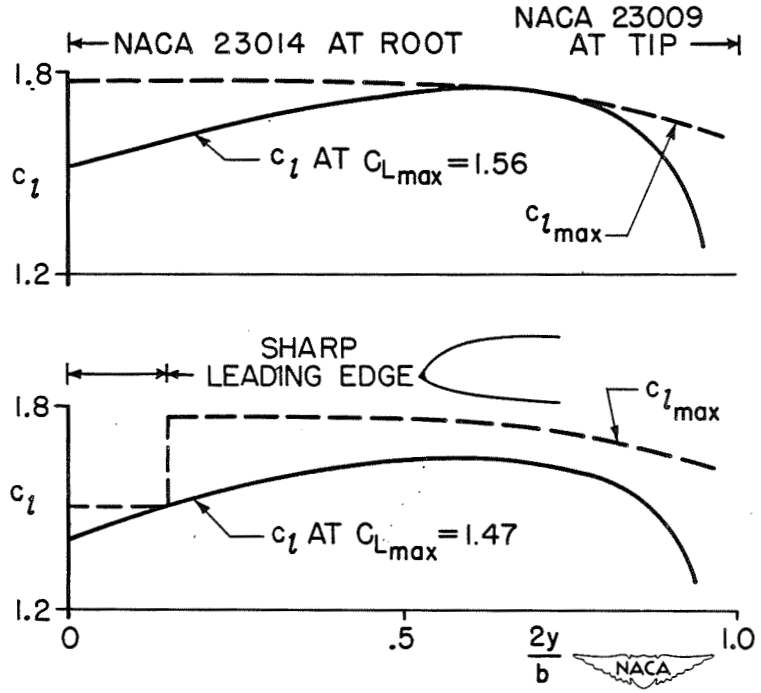

Figure 6.- Effect of a sharp leading edge on the calculated stalling characteristics of a wing.

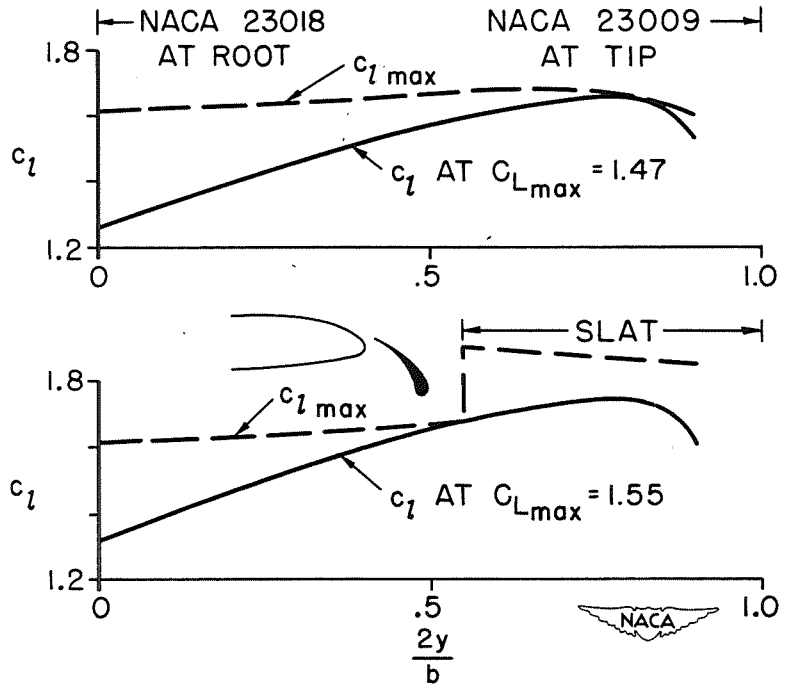

Figure 7.- Effect of leading-edge slats on the calculated stalling characteristics of a wing.

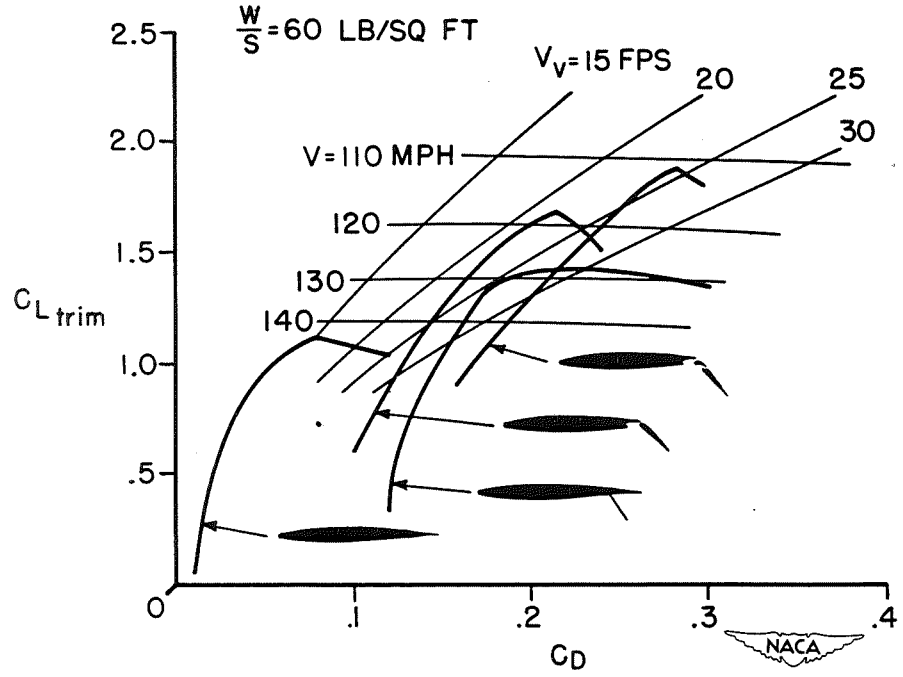

Figure 8.- Effect of split, single slotted, and double slotted flaps on the lift-drag characteristics of a wing with NACA 65-210 airfoil sections.

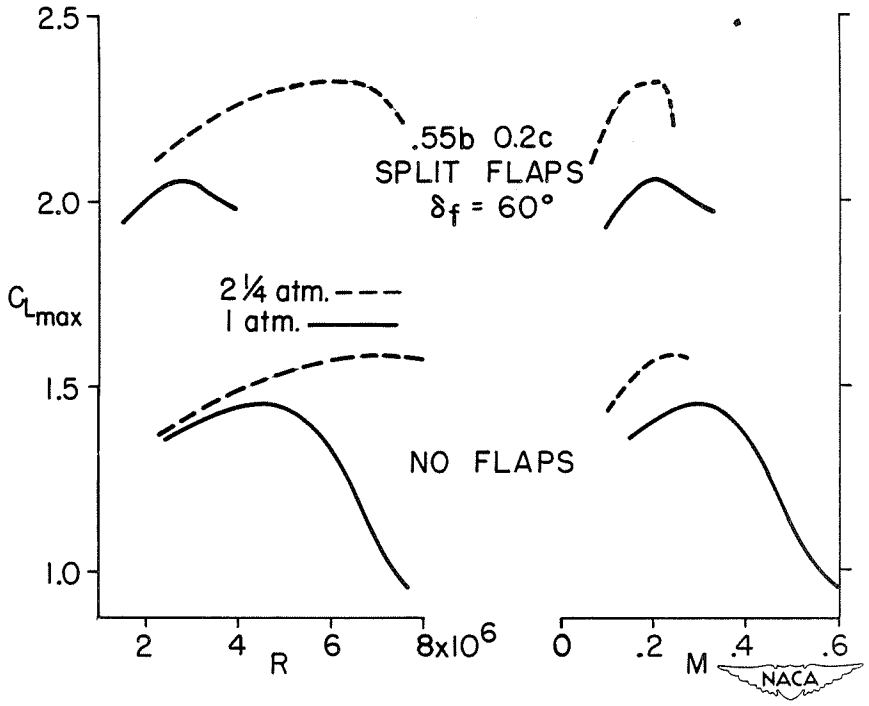

Figure 9.- Effect of Reynolds number and Mach number on the maximum lift coefficient of a wing with NACA 230-series airfoil sections.

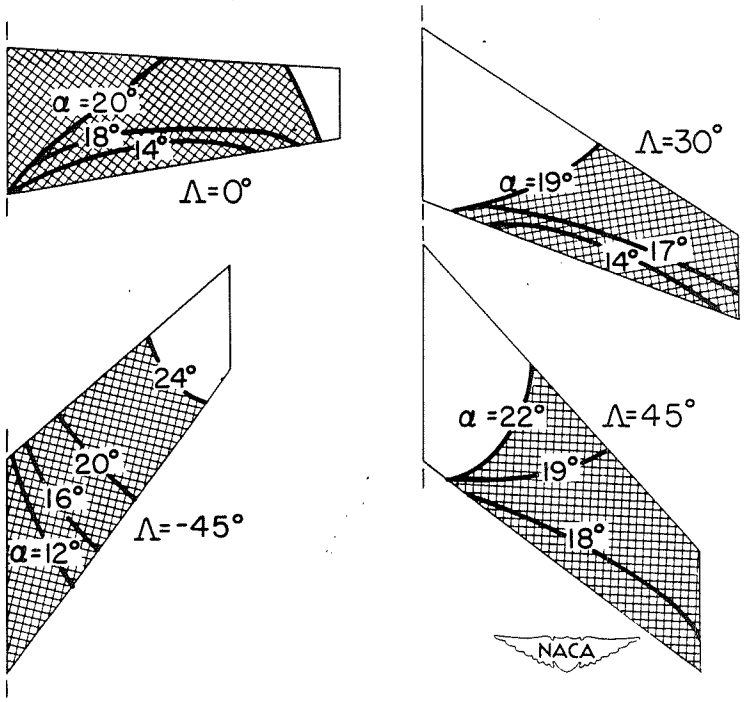

Figure 10.- Stall progressions for wings with and without sweep.

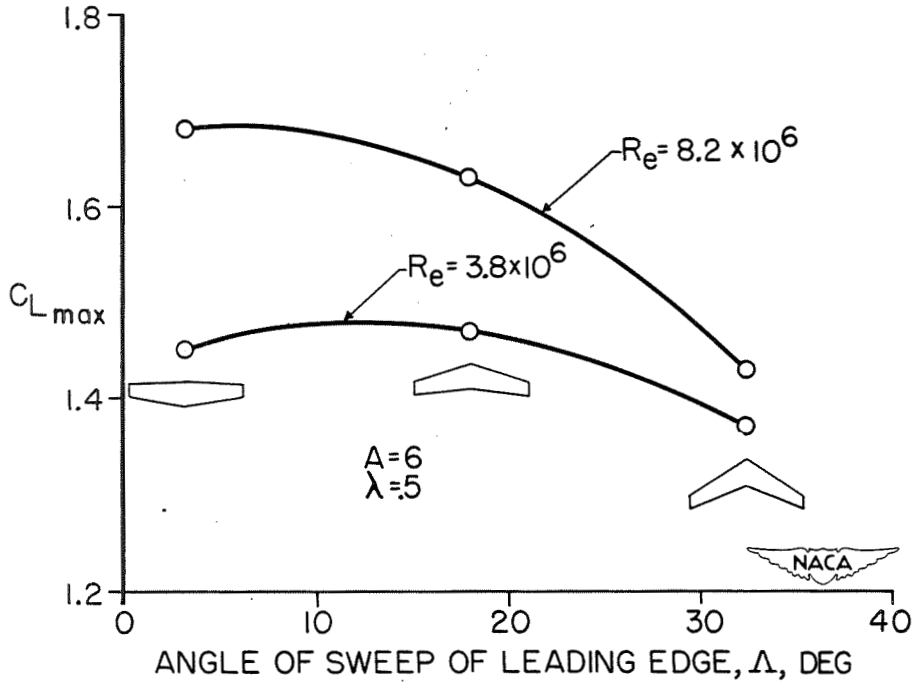

Figure 11.- Effect of sweep on the maximum lift coefficients of wings.

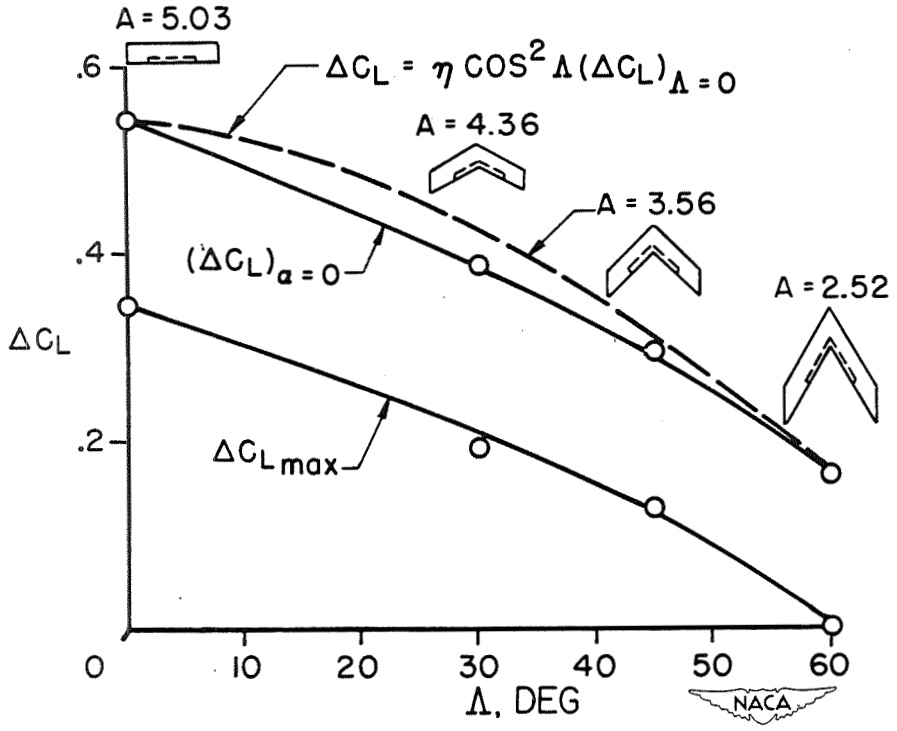

Figure 12.- Effect of sweep on the increment in lift coefficient due to flaps.

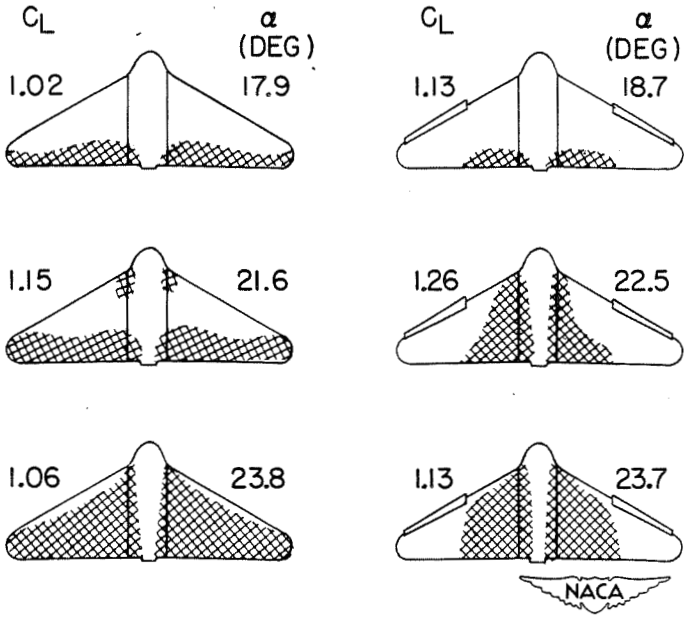

Figure 13.- Effect of leading-edge slats on the stalling characteristics of a sweptback wing.